CHAPTER II

SULFUR- AND WATER-TOLERANCE OF Pt/KL AROMATIZATION CATALYSTS PROMOTED WITH Ce AND Yb

Siriporn Jongpatiwut, Paneeya Sackamduang,
Thirasak Rirksomboon, and Somchai Osuwan

The Petroleum and Petrochemical College,
Chulalongkorn University, Bangkok, Thailand

Walter E. Alvarez and Daniel E. Resasco*

School of Chemical Engineering and Materials Science,
The University of Oklahoma, Norman, OK 73019

*To whom correspondence should be addressed: e-mail: resasco@ou.edu

Abstract

Different Pt/KL catalysts containing rare earth (RE; Ce and Yb) promoters were prepared by two techniques, incipient wetness impregnation (IWI) and vapor phase impregnation (VPI). The catalysts were tested for the activity and the selectivity of *n*-hexane aromatization to benzene under clean, sulfur-containing, and water-containing feeds at 500°C. It was observed that the catalysts prepared by the VPI technique exhibited much higher activity and selectivity than those prepared by IWI. It was also found that although under clean conditions, the addition of Ce or Yb caused a decrease in activity, in the presence of sulfur the addition of Ce and to a lesser extent Yb, significantly inhibited catalyst deactivation.

The influence of water in the feed was investigated by contacting the catalysts for 1 h to a feed containing 3 mol. % water. After this treatment, all the catalysts exhibited a significant activity loss. This loss is more pronounced for the catalyst prepared by the VPI method. The catalyst prepared by IWI already had suffered a significant deactivation before the water treatment, so the activity drop was not so pronounced. The sample prepared by VPI not only showed a drop in activity immediately after the water treatment but it became more susceptible to deactivation afterwards. By contrast, the Ce-promoted catalyst showed a more stable activity after the treatment.

All catalysts were characterized before and after reaction by a number of techniques. In agreement with previous studies, FT-IR of adsorbed CO and chemisorption results indicated that the VPI method resulted in higher Pt dispersion than that obtained by the IWI method. After reaction in the presence of sulfur, the Ce-promoted Pt/KL catalyst showed a higher resistance to metal agglomeration and a lower rate of coke formation than the unpromoted Pt/KL. On all the catalysts, the amount of carbon deposits was greater in the presence of sulfur and after exposure to water vapor than under reaction was clean feeds. This difference is explained in terms of metal particle growth and location in the zeolite.

Introduction

The exceptionally high activity and selectivity of Pt/KL catalysts for *n*-hexane aromatization have been known for two decades and form the basis of a commercial process [1, 2]. A shortcoming of these catalysts is their extremely high sensitivity to even traces of sulfur (e. g. parts per billion) [3]. Acceptable aromatization performances can only be achieved by reducing the sulfur concentration in the feed to extremely low levels, which significantly raises the cost of the process. Therefore, the development of Pt/KL catalysts able to withstand higher sulfur concentrations than those used today appears as an attractive goal [4]. In previous work, sulfur poisoned Pt/KL catalysts have been characterized by TEM [4, 5], EXAFS [4, 6], and diffuse reflectance infrared Fourier transform spectroscopy (DRIFTS) of adsorbed CO [2, 7, 8]. Those studies demonstrated that Pt particle growth is accelerated in the presence of sulfur, leading to zeolite pore plugging and significant losses in catalytic activity.

There have been several attempts to increase the sulfur-tolerance of the catalyst. While some researchers have investigated different methods of preparation and pretreatment [9-11] others have tried to add promoters to increase the resistance to sulfur [3, 12-15]. For example, Fang, *et al.* [12,16] demonstrated that the addition of rare earth (RE) to Pt/KL catalysts prepared by liquid impregnation could increase the sulfur resistance and aromatization selectivity. More recently, Jacobs *et al.* [7, 17] pointed out that the preparation method affects the morphology and size of Pt clusters. They demonstrated that the Pt/KL prepared by the vapor phase impregnation (VPI) previously used by Hong *et al.* [18] and Bellatreccia *et al.* [19] exhibited a higher fraction of small metal particles inside the zeolite channel than those prepared by the conventional incipient wetness impregnation (IWI). The size and morphology of the platinum clusters resulting from the VPI preparation method were proposed to be responsible for the improved catalytic performance of these samples, both under clean and sulfur-containing feeds. Moreover, these authors showed that the combined effects of the preparation method and the addition of Tm as a promoter resulted in a catalyst with improved Pt dispersion, aromatization

activity, and sulfur-tolerance [7, 15]. Although, as shown in the patent literature [20, 21] it may be possible to obtain high dispersions from a liquid/solid preparation method, in our hands, the best metal dispersion and homogeneity has always been achieved by using the VPI method [17].

In this contribution, we have expanded those studies to other rare earth elements (Ce and Yb), using the preferred VPI preparation method. As before, these catalysts were compared under clean and sulfur-containing feeds. At the same time, it is well known among industrial practitioners that the aromatization Pt/KL catalysts are very sensitive to water vapor. Therefore, the resistance to deactivation by treatment in a feed containing 3 mol. % water vapor was studied on these novel catalysts in comparison to standard Pt/KL. All the fresh (reduced) samples as well as samples spent under various conditions were characterized by a combination of techniques including FT-IR of adsorbed CO, EXAFS/XANES, temperature programmed oxidation (TPO), and hydrogen chemisorption.

Experimental

1. Catalyst Preparation

Unpromoted 1 wt. % Pt / KL catalysts and rare earth-promoted catalysts were prepared by two methods, IWI and VPI. The KL zeolite (K-LTL, BET area, 292 m^2g^{-1}, SiO_2/Al_2O_3 ratio = 6) was provided by Tosoh Company. Before adding the metals, the zeolite was dried in an oven at 110°C for 12 h and calcined at 350°C in flow of dry air of 100 $cm^3(min\ g_{cat})^{-1}$ for 5 h.

The liquid to solid ratio used in the IWI preparations was adjusted to 0.69 cm^3 $(g_{zeol})^{-1}$ in order to obtain incipient wetness conditions. In this type of preparation, the platinum precursor used was tetraamine platinum (II) nitrate (from Alfa Aesar). Proper amounts of tetraamine platinum (II) nitrate were weighted and dissolved in deionized water and then impregnated in the dried support by slowly adding drops of solution under an inert atmosphere of He. Next, the mixture was dried at room

temperature for 4 h before drying in an oven at 110°C overnight. After cooling, the mixture was calcined at 350°C in flow of dry air at 100 cm^3(min g$_{cat}$)$^{-1}$ for 2 h.

For the VPI method, the metal precursors were platinum (II) acetyl-acetonate (from Alfa Aesar), cerium (2,4-pentanedionate; from Alfa Aesar), and ytterbium (2, 4-pentanedionate; from Alfa Aesar). The catalysts were prepared by physically mixing the weighed metal precursors and the calcined support under inert atmosphere of He. The mixture was then heated up slowly to 40°C and held at that temperature for 3 h, heated again to 60°C holding it for 1 h, and further heated to 100°C, at which temperature the mixture was held for 1 h to complete the sublimation of the metal precursor. After sublimation, the mixture was heated under flowing He to 130°C and held for 15 min. In the last step, the mixture was calcined at 350°C in flow of dry air at 100 cm^3(min g$_{cat}$)$^{-1}$ for 2 h. In the rare earth-containing samples, prior to the loading of the Pt precursor, the RE/KL support was prepared using the same VPI and calcination procedure as described for the loading of Pt, using the same temperatures and heating times. As described in a previous report [17], by conducting the VPI under He flow instead of under vacuum, a small fraction of the impregnating metals (about 10%) is lost in the process, but the dispersion and homogeneity of the catalyst are very similar to that obtained by VPI under vacuum.

2. Catalytic Activity Measurements

The catalytic activity measurements were conducted in a fixed-bed, continuous flow reactor. The reactor consisted of 0.5 in. stainless steel tube with an internal K-type thermocouple. To avoid unwanted contamination, independent systems were used for runs using clean feeds and runs with sulfur-containing feeds. n-Hexane (from Merck) was injected to the system via a T-junction by using a syringe pump. The tubes and fittings beyond the T-junction were heated in order to prevent any n-hexane condensation. Reactions were performed at atmospheric pressure and 500°C. The WHSV used was 5 h^{-1}. The hydrogen: n-hexane molar ratio was kept at 6:1, employing 0.4 g of catalyst in each run. Prior to the reaction, the catalyst was slowly heated in a 100 cm^3(min g$_{cat}$)$^{-1}$ flow of H$_2$ up to 500°C and held at that temperature

for 1 h. For the sulfur deactivation studies, thiophene was pre-mixed in *n*-hexane at the appropriate concentration to obtain 2.5 ppm S in the reaction mixture. For the hydrothermal stability studies, water was injected during 1 h by passing the carrier hydrogen through a water saturator kept at room temperature. The *n*-hexane feed was then injected into the hydrogen/water stream through a syringe pump prior to entering the reactor keeping a water-to-*n*-hexane molar ratio of 1:5 for 1h. After this treatment, the dry feed was resumed.

The products were analyzed in a Shimadzu GC-17A equipped with a capillary column HP-Plot/Al$_2$O$_3$ "S" deactivated. The activity data are reported in terms of total hexane conversion and product selectivity, which is defined as the moles of each individual product per mole of hexane converted.

3. Catalyst Characterization

3.1 Hydrogen Chemisorption: The hydrogen uptake on fresh (reduced) catalysts was determined in a Pyrex static volumetric adsorption system, equipped with a high capacity, high vacuum pump that provided clean vacuum on the order of 10^{-9} Torr. Prior to each experiment, 0.4 g of dried fresh catalyst was reduced in situ at 500°C for 1 h under flowing H$_2$, cooled down to 300°C, evacuated to 10^{-7} Torr at 300°C for 20 min, then cooled down to room temperature under vacuum. Adsorption isotherms were obtained from several adsorption points ranging from 0 to 100 Torr and the final H/Pt value determined by extrapolation to zero pressure.

3.2 Diffuse Reflectance Infrared Fourier Transform Spectroscopy (DRIFTS) of Adsorbed CO: The fresh and spent Pt/KL and Pt/RE-KL catalysts were characterized using CO as a probe in a Bio-Rad FTS-40 DRIFTS spectrometer, equipped with a MCT detector and a diffuse reflectance cell type HVC-DR2 from Harrick Scientific, with ZnSe windows. Each sample was reduced in situ in flow of H$_2$ at 300°C for 1 h, purged in He for 30 min at room temperature. The background spectrum for each sample was obtained after this treatment, before exposure to CO. The catalyst was then exposed to a flow of 3 % CO in He for 30 min and purged in

He for 30 min. Subsequently, the spectrum for adsorbed CO was obtained at a resolution of 8 cm^{-1} averaging 128 scans.

3.3 X-ray Absorption Analysis (XANES and EXAFS): The absorption spectra at the Pt L$_2$ (13,273 eV) and L$_3$ (11,564 eV) edges for fresh and spent Pt/KL and Pt/Ce-KL catalysts were measured using a Si(111) crystal monochromator at line X-18B, at the National Synchrotron Light Source (NSLS) at Brookhaven National Laboratory, Upton, NY. The X-ray ring at the NSLS has an energy of 2.5 GeV and ring current of 80-220 mA. The measurements were conducted in a stainless steel sample cell that allowed in situ pretreatments at temperatures ranging from liquid nitrogen to 500°C. Prior to each measurement, the catalysts, previously reduced ex situ at 500°C, were re-reduced in situ at 300°C (heating rate of 10°C min^{-1}) for 30 min in flowing H$_2$. After the reduction step, the sample was cooled down under flowing He. The X-ray absorption spectra were recorded at liquid nitrogen temperatures under He flow. Six scans were recorded for each sample. The average spectrum was obtained by adding the six scans. The pre-edge background was subtracted by using power series curves. Subsequently, the post-edge background was removed using a cubic-spline routine. The spectra were normalized to the height of the adsorption edge. The range in k-space used for the analysis was 3.0 - 15 A^{-1}. To avoid overemphasizing the low energy region the χ-data were k^3-weighted [22]. Absorption data obtained on a Pt foil at liquid nitrogen temperature was used as an experimental reference for the Pt-Pt bond (coordination number, CN = 12; R = 0.275 nm).

3.4 Temperature Programmed Oxidation (TPO): Temperature programmed oxidation was employed to analyze the amount and characteristics of the coke deposits over spent catalysts. TPO of the spent catalysts were performed in a ¼ in. quartz fixed-bed reactor under continuous flow of 5% O$_2$/He, increasing the temperature at a linear heating rate of 12°C min^{-1}. The spent catalysts were dried overnight at 110°C before weighing 30 mg of sample and supporting it on quartz wool inside the quartz tube. The catalysts were then exposed to the 5% O$_2$ in He mixture for 30 min at room temperature and subsequently the heating ramp was

started. The CO_2 produced by the oxidation of coke species was monitored in a mass spectrometer. The amount of coke was calibrated by using 100 µl pulses of pure CO_2. The partial pressure of evolved CO_2 was normalized to the total pressure and the maximum signal in the pulses of CO_2

Results and Discussion

1. Catalytic Activity Measurements

1.1 Clean n-Hexane Feed: The Pt/KL (IWI), Pt/KL (VPI) and Pt/RE-KL (VPI) were tested for the aromatization of *n*-hexane as a function of time on stream. The *n*-hexane conversion and selectivity to benzene, obtained with a clean *n*-hexane feed during a 30 h run, are reported as a function of time on stream in Fig. 1a and b, respectively. In agreement with previous investigations, the VPI catalysts were more resistant to deactivation than the IWI catalysts. At the same time, the selectivity towards benzene was consistently higher on the VPI catalysts than on the IWI catalysts. It was found that when using clean *n*-hexane feed, the addition of 0.15% Ce or Yb to the VPI catalysts caused a decrease in activity and no significant change in benzene selectivity. However, the rate of deactivation was less pronounced with the clean feed and most important, as shown next, the addition of Ce had a positive impact on sulfur-tolerance. In previous studies [7] we found that the addition of Tm caused an increase in benzene yield, with both clean and sulfur-containing feeds. So, it is apparent that the role of Ce (or Yb) is somewhat different from that of Tm.
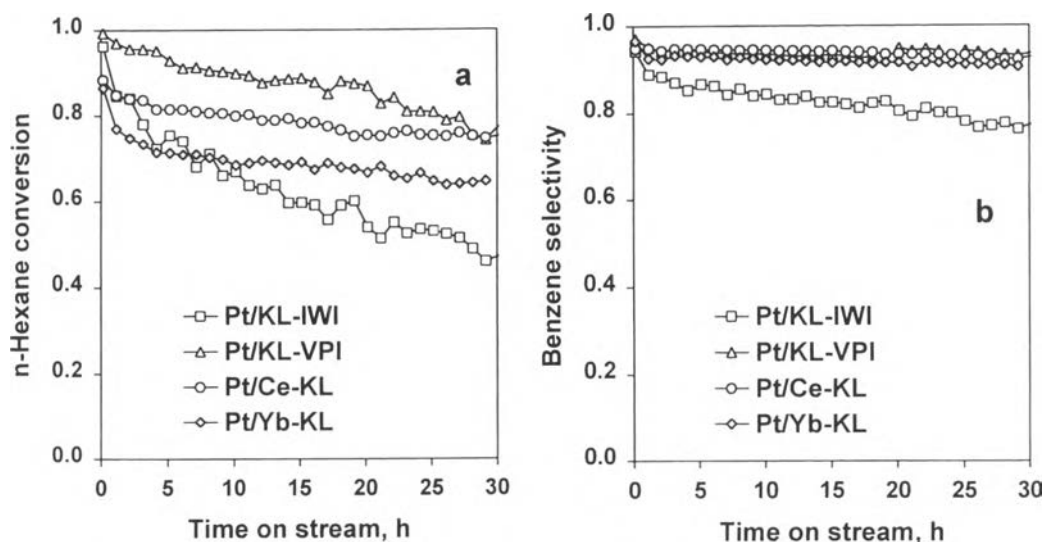
Fig. 1. *n*-Hexane conversion (a) and benzene selectivity (b) vs. time on stream under clean *n*-hexane feed over various Pt/KL and rare earth-promoted Pt/KL catalysts. Reaction conditions: WHSV= 5 h^{-1}; H$_2$/*n*-hexane molar ratio = 6; temperature = 500°C.

1.2 Sulfur Containing Feed: As mentioned earlier, the high sensitivity to sulfur is a known problem of Pt/KL catalysts. They are much more sensitive to sulfur than conventional bifunctional reforming catalysts [23]. In order to study the sulfur-tolerance of different Pt/KL catalysts, 2.5 ppm sulfur was added to the feed. The *n*-hexane conversion and product selectivity are shown in Fig 2a and b, respectively, as a function of time on stream. It is observed that, in the presence of sulfur, the total conversion and benzene selectivity dramatically dropped on all catalysts in comparison to those in the clean runs. It was observed that in the presence of sulfur, the Pt/KL (VPI) catalyst showed higher activity and selectivity than the IWI catalyst during the first 15 h. After that period of time, both catalysts deactivate to a similar extent. Interestingly, although under the clean feed, Pt/RE-KL showed lower activity than the unpromoted VPI catalyst, in the presence of sulfur, the Pt/RE-KL exhibited higher activity, selectivity, and stability than the unpromoted catalyst, with a clear advantage for the Ce-promoted catalyst in comparison to the one promoted with Yb. Of course, when comparing the different effects of Ce and Yb, we must note that for the same weight loading (0.15 wt.%), the molar concentration of Ce is almost 25%

higher than that of Yb. However, as discussed next, we may not expect an improved catalytic performance if the Yb loading were increased.
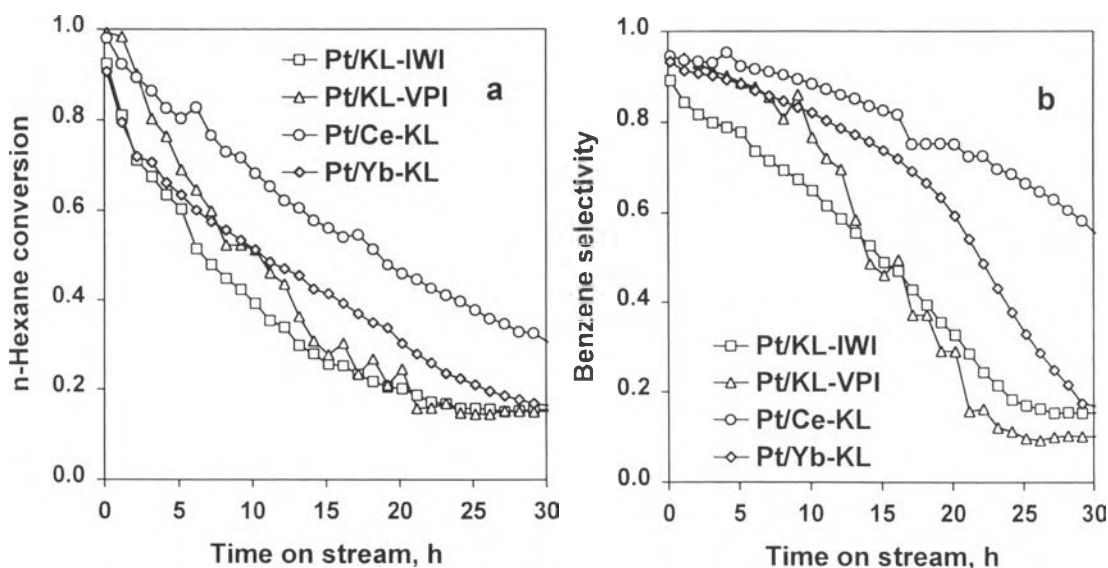

Fig. 2. *n*-Hexane conversion (a) and benzene selectivity (b) vs. time on stream under 2.5 ppm sulfur containing feed. Reaction conditions: WHSV= 5 h^{-1}; H$_2$/*n*-hexane molar ratio = 6; temperature = 500°C.

At the same time, as previously observed [4] the selectivity towards hexenes (Fig. 3a) greatly increased with time on stream. Another significant trend appears in the selectivity to pentanes, which reflects the changes in hydrogenolysis activity of the catalysts under sulfur. As shown in Fig. 3b, the percentage of pentanes in the product initially increased, reached a maximum and then decreased in all the catalysts. However, important differences where observed in the times at which this maximum was reached. For the unpromoted VPI and IWI catalysts, the maximum was reached after a relatively short time on stream, i.e. around 13 h. By contrast, the promoted catalysts required much longer times to reach the maximum, i.e. 25 h for the Yb-promoted catalyst and 43 h (not shown) for the Ce-promoted catalyst. It is generally accepted that the hydrogenolysis products are mainly formed when large metal ensembles are present. Therefore, the observed initial increase in hydrogenolysis activity would be consistent with a sulfur-assisted Pt agglomeration as previously proposed [5, 6]. On the other hand, the hydrogenolysis activity drop after the maximum could be ascribed to sulfur poisoning of the Pt surface that would

become apparent only at longer times, when the sulfur concentration builds up on the Pt surface. Noteworthy, this poisoning not only inhibits hydrogenolysis, but also the aromatization activity. As demonstrated on a study on a Pt(111) crystal [24] both *n*-hexane aromatization and hydrogenolysis on clean Pt surfaces require a large ensemble of atoms and are similarly affected by poisoning. According to this explanation, the more rapid increase in hydrogenolysis observed initially on the unpromoted catalysts would indicate that the addition of the RE inhibits the rate of Pt agglomeration. A slower agglomeration results in a slower increase in pentane production, as seen in the figure for the RE-promoted catalysts. This inhibition can be due to two possible causes: (a) the RE oxides prevent Pt agglomeration by acting as anchoring sites for Pt, or (b) the RE oxides themselves act as sulfur getters. The fact that the maxima on the RE-promoted catalysts occur after longer times on stream supports the second possibility. That is, the RE oxides scavenge sulfur, thus keeping the Pt surface free of sulfur for longer times. It is known that Ce oxide can react with sulfur-containing compounds and effectively trap sulfur [25]. Although this reaction requires high temperature, it may be accelerated by the presence of carbon [26]. A simple calculation can be made comparing the amount of sulfur fed to the reactor and the amount of Ce present on the catalyst. For example, on a 0.4 g catalyst sample containing 0.15 wt. % Ce, the total amount of Ce is 4.3×10^{-6} mol. Using feed containing 2.5 ppm S, a corresponding amount of sulfur would be build up in about 28 h if all the sulfur sent to the reactor is trapped by the catalyst. In fact, it is suggestive that the greatest resistance to deactivation by sulfur is seen in the Ce-promoted catalyst during the first 15-20 h. Beyond that time, the rate of deactivation is similar to that of the unpromoted catalyst while at around that time, a break in benzene selectivity is observed.
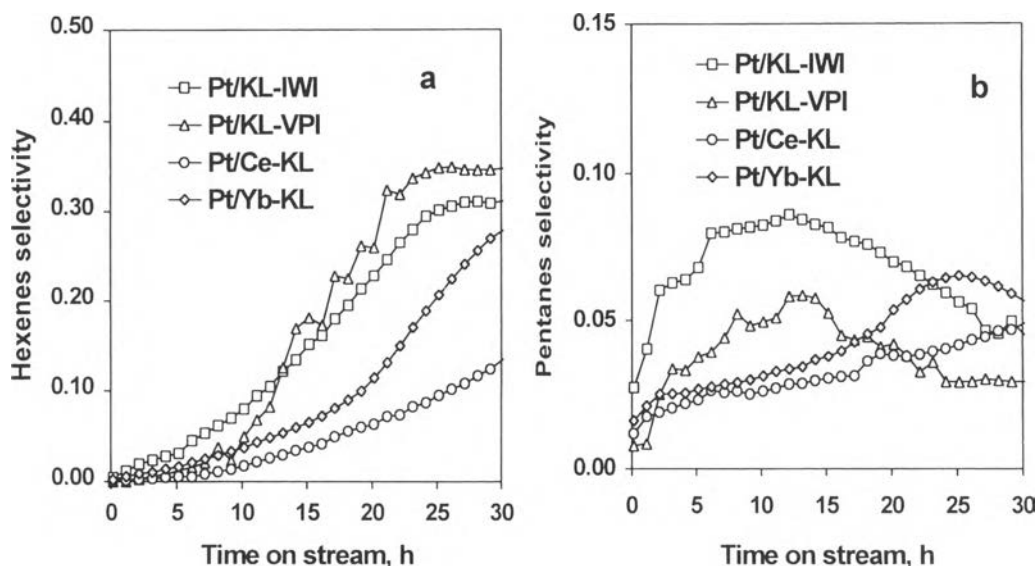
Fig. 3. Hexenes selectivity (a) and C5 selectivity (b) vs. time on stream under 2.5 ppm sulfur containing feed. Reaction conditions: WHSV= 5 h^{-1}; H$_2$/n-hexane molar ratio = 6; temperature = 500°C.

Table 1 summarizes the product distribution obtained after 9 h on stream on the unpromoted Pt/KL(VPI) and the Ce-promoted Pt/KL(VPI) catalyst. The product distribution is very similar and shows that the dominant product is benzene, with hexenes as the most abundant by-products. Very little methyl-cyclo-pentane, and methyl pentanes were formed. As we have reported before [4], the low selectivity towards these by-products is kept even at near-zero conversions. In earlier studies much higher selectivities towards methyl-cyclo-pentane and methyl pentanes have been reported, but we believe that they arise from secondary isomerization on residual acid sites. When the Pt/KL catalyst contains no acidity no isomerization products are observed. Also, only C6 ring-closure products are generated. As pointed out by Davis [27], at low-to-moderate pressures if C5 ring-closure intermediates are formed they will not leave the surface and most probably end up as coke. The important point to emphasize here is that the addition of Ce had important consequences on the level of activity and stability, but no much effect on product distribution. This may be taken as an indication that the acidity of the zeolite may have not changed significantly by the incorporation of the Ce.

Table 1

Product distribution of *n*-hexane aromatization on Pt/KL and Pt/Ce-KL catalysts using clean and 2.5 ppm sulfur-containing feeds, after 9 h on stream. Reaction conditions: 500°C, H_2:*n*-C_6 ratio 6:1, WHSV 5 h^{-1}

	Clean Feed			2.5 ppm S Feed		
	Pt/KL (IWI)	Pt/KL (VPI)	Pt/Ce-KL	Pt/KL (IWI)	Pt/KL (VPI)	Pt/Ce-KL
Conversion (%) Product Selectivity (%)	66.0	90.3	80.6	42.3	57.3	71.7
C1-C5	6.9	4.3	3.6	13.5	6.0	5.5
MCP	0.9	0.4	0.2	0.7	0.7	0.4
2-MP	0.4	0.5	0.05	0.3	0.3	0.2
3-MP	0.3	0.4	0.05	0.3	0.3	0.2
Benzene	83.9	93.7	94.5	67.4	86.0	89.3
Hexenes	7.6	0.7	1.5	17.8	6.6	4.2

1.3 Water Vapor-Containing Feed: To study the effect of water addition to the Pt/KL and Pt/RE-KL catalysts, after an initial reaction period of 9 h under dry *n*-hexane feed, water vapor was injected in the feed for 1 h, at a molar concentration of 3 %. After this period, the reaction was continued with dry feed for an additional period of 20 h. Fig. 4 shows the conversion and selectivity data as a function of time on stream before and after the water injection. It can be seen that all catalysts exhibited a clear drop in both, conversion (Fig. 4a) and benzene selectivity (Fig. 4b) after the exposure to water vapor. It is interesting to note that the exposure to water not only caused a drop in activity, which was immediately apparent after resuming the reaction, but also caused a change in the rate of deactivation. This deactivation was affected by the presence of RE. As seen in the figure, although after the water treatment the Ce-containing catalyst showed decreased conversion and decreased selectivity, they remained rather constant during the second dry period. By contrast, with the unpromoted catalyst, the rate of deactivation after the water addition was much more pronounced.
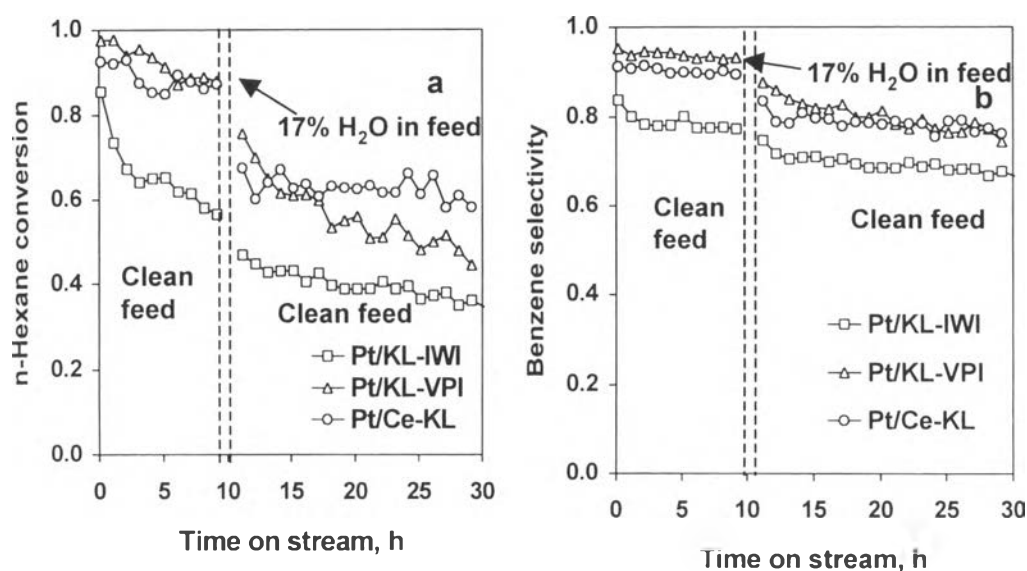
Fig. 4. *n*-Hexane conversion (a) and benzene selectivity (b) vs. time on stream first 9 h in clean *n*-hexane feed, then in the presence of 3 mol. % water vapor containing *n*-hexane feed for 1 h, and then continue in clean *n*-hexane feed. Reaction conditions: WHSV= 5 h^{-1}; H$_2$/*n*-hexane molar ratio = 6; temperature = 500°C.

On all catalysts, the drop in conversion and benzene selectivity was accompanied by an increase in the production of hexenes and C1-C5 fragments. As demonstrated in our previous work [4, 8], when Pt particles grow outside the channels of the zeolite, both hexenes and C1-C5 products greatly increase. Therefore, it can be concluded that the main consequence of the exposure to water is an enhancement in Pt particle growth.

Interestingly, the activity drop caused by exposure to water was much more pronounced on the unpromoted VPI catalyst than on the unpromoted IWI catalyst. It appears that in the absence of a RE promoter, the presence of water destabilizes the small clusters, which otherwise would be very stable inside the zeolite, either under clean feeds [18] or in the presence of sulfur [7, 8]. On the other hand, these results show that the RE-promoted catalysts not only exhibit a superior tolerance to sulfur, but also to the water exposure. This tolerance, together with the higher stability exhibited in the clean run, demonstrate that the role of Ce is not merely due to its ability to scavenge sulfur, but also to an interaction with Pt making it less susceptible

to sintering. We will explore this effect in the next section when we discuss the role of Ce in the enhancement of the metal-support interactions.

2. Catalyst Characterization

2.1 Hydrogen Chemisorption: Hydrogen uptakes on all reduced fresh catalysts are listed in Table 2. As previously observed [4, 8] the catalysts prepared by VPI exhibit higher H/Pt values than those prepared by the IWI method. On the other hand, the addition of rare earth oxides results in lower uptakes on the promoted catalysts than on the unpromoted catalysts, which parallel the catalytic activity data obtained with the clean feed (see Fig. 1a), which showed lower conversions on the RE-promoted catalysts. Seeing that the addition of RE did not have any noticeable effect on selectivity, we infer that the losses in hydrogen uptake and conversion may be related to some pore blockage by RE oxide and Pt entombment inside the plugged channels of the zeolite. This blockage would not affect the metal particle size, but it would render a fraction of the particles inaccessible to the gas. Therefore, lower H/Pt values on the RE-promoted catalysts not necessarily imply larger Pt particles. In line with this possibility, it was observed that when the RE concentration was increased from 0.15 wt. % Ce to 0.25 wt. % Ce, the hydrogen uptake further decreased.

Table 2

Hydrogen chemisorption data on fresh (reduced) catalysts

Catalyst	H/Pt
Pt/KL (IWI)	0.56
Pt/KL (VPI)	0.91
Pt/Ce (0.15%)-KL (VPI)	0.86
Pt/Ce (0.25%)-KL (VPI)	0.80
Pt/Yb-KL (VPI)	0.83

2.2 DRIFTS of Adsorbed CO: FT-IR of adsorbed CO on the fresh (reduced) Pt/KL and Pt/RE-KL catalysts are shown in Fig. 5. As described in our previous reports [7, 8], during the adsorption of CO on highly dispersed Pt clusters in KL zeolites formation of Pt carbonyls occurs. These carbonyls, which result from a disruption of the Pt clusters by interaction with CO, are stabilized inside the L-zeolite channels and exhibit characteristic IR absorption bands below 2000 cm^{-1}. Given that these carbonyls can only be formed from very small Pt clusters and can only be stabilized inside the zeolite [28], we have previously used the presence of this band as an indication of the presence of very highly dispersed Pt clusters inside the zeolite. By contrast, when the catalyst contains Pt particles located outside the channels of the zeolite, a clear shoulder is evident at 2070 cm^{-1}. The bands between 2050 and 2000 cm^{-1} were related to CO adsorbed on particles near the pore mouth. In this case, only small shoulders at 2070 cm^{-1} were observed for all of the catalysts, even for the one prepared by IWI. According to our previous studies [7, 8, 17], this would indicate that all of the samples are well prepared, but those prepared by VPI have a larger fraction in the smallest size range inside the zeolite, which in the presence of CO appear as Pt carbonyls. In fact, the characteristic broad band centered at 1970 cm^{-1} was clearly evident for the Pt/KL and Pt/RE-KL catalysts prepared by the VPI method. It is suggestive that the intensity ratio of the band at 1970 cm^{-1} to that at 2050 cm^{-1}, is significantly lower for the Pt/KL catalyst prepared by the IWI method than for any of the VPI catalysts. Accordingly, the DRIFTS spectra give further evidence that the VPI method results in a higher metal dispersion than the IWI method as previously proposed [8]. The small but clear band at 2070 cm^{-1} would indicate that the fraction of exposed Pt particles outside the zeolite is relatively small. So, it is likely that the IWI catalyst have a small number of relatively large Pt clusters outside the zeolite. An important conclusion can be reached in this sense regarding the RE-promoted catalyst. That is although the hydrogen uptake (H/Pt) values obtained on the RE-promoted catalysts were lower than those on the unpromoted Pt/KL, the DRIFTS spectra indicate that the former catalysts have, at least, the same high degree of metal dispersion as the latter, given that the band ascribed to Pt carbonyls is very strong in comparison with the bands ascribed to CO adsorbed on larger particles. Also, the band at 2070 cm^{-1}, characteristic of Pt outside the zeolite

channels, on these VPI-promoted catalysts was even smaller than that for the unpromoted catalysts. In line with this result and as discussed next, EXAFS data show that indeed the Pt particle size on the Pt/KL (VPI) and Pt/Ce-KL are almost identical.
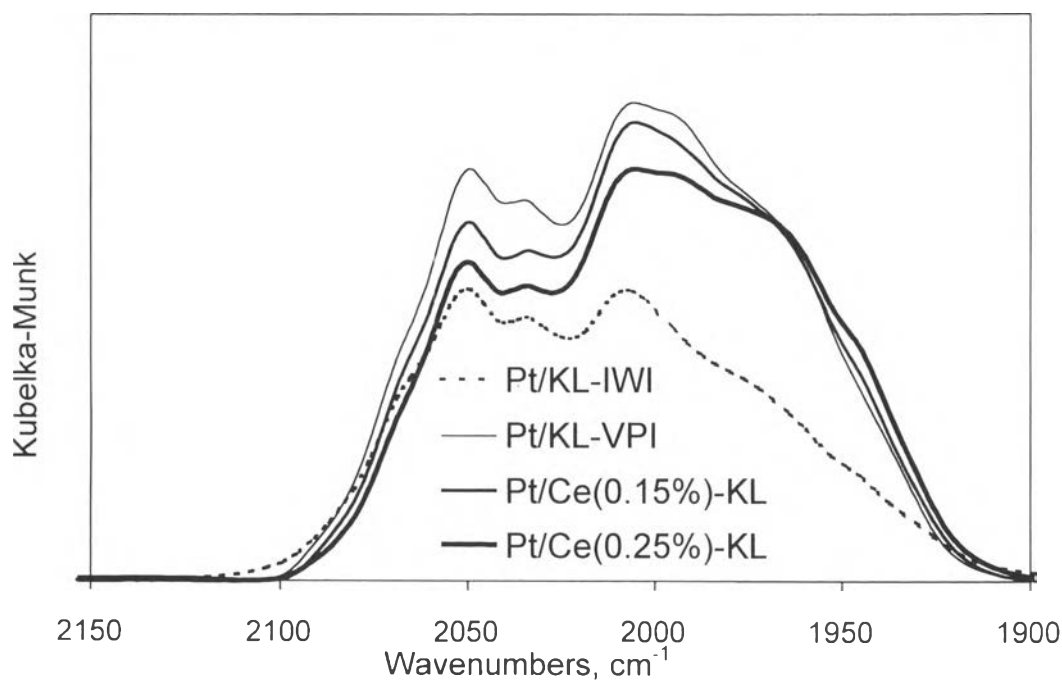

Fig. 5. DRIFTS of CO adsorbed on fresh catalysts reduced in situ at 300°C after an ex situ reduction at 500°C. The reduced catalysts were exposed to a flow of 3% CO in He for 30 min at room temperature and purged in He for 30 min.

In agreement with this conclusion, the activity data showed that although the total *n*-hexane conversion on the Pt/RE-KL catalyst was lower than on the unpromoted catalysts, the benzene selectivity was similar, and as demonstrated in previous work, when catalysts contain a significant fraction of metal particles in the form of large aggregates outside the channels of the zeolite, the formation of olefins increases and the benzene selectivity greatly decreases. None of these characteristic trends was observed on the Ce-promoted catalyst, showing that it did not contain large Pt aggregates.

DRIFTS of adsorbed CO has also been used to compare the state of the catalyst before and after reaction with the sulfur-containing feed. As shown in Fig. 6, the

intensities of all bands observed for the sulfur poisoned catalysts were significantly lower than those for the reduced fresh catalyst. However, the drop in the band intensity observed for the Pt/Ce-KL after sulfur poisoning for 54 h (Fig. 6b) was much less pronounced than that on the unpromoted catalyst poisoned for 40 h (Fig. 6a). As mentioned previously, the greater tolerance to sulfur exhibited by the Ce-promoted catalyst can be due to either the ability of the rare earth to effectively anchor the Pt particles, preventing agglomeration, or to a direct interaction of the RE with sulfur, thus acting as a sulfur getter. The sulfur-scavenging ability of Tm was previously demonstrated by Jacobs *et al.* [7] for the case of Pt/Tm-KL catalysts. It is possible that Ce exhibits a similar ability.
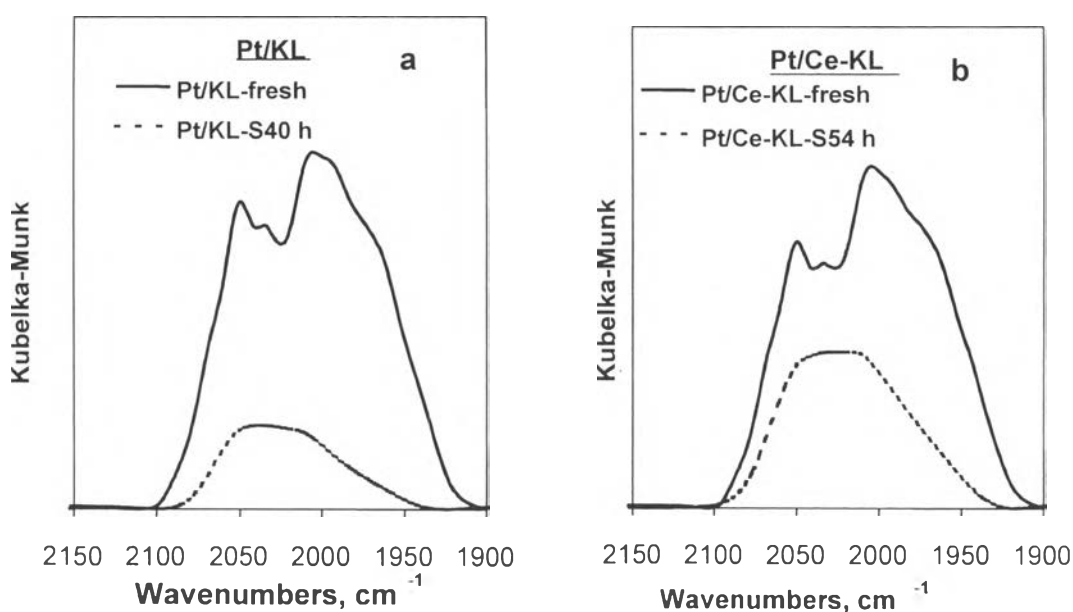
Fig. 6. DRIFTS of CO adsorbed on (a) Pt/KL and (b) Pt/Ce-KL fresh and after reaction with 2.5 ppm sulfur containing feed for 30 h. Each sample was reduced in situ at 300°C. The reduced catalysts were exposed to a flow of 3% CO in He for 30 min at room temperature and purged in He for 30 min.

2.3 TPO Profiles of Spent Catalysts: To quantify the amount of coke deposited during the reaction and obtain information about how the coke distributes over the catalyst, TPO of the carbonaceous deposits were conducted on all the spent catalysts. The TPO profiles obtained after reaction with feeds containing sulfur over Pt/KL and

Pt/Ce-KL catalysts are illustrated in Fig. 7a and b. The total amounts of carbon in each sample has been included in the figures next to the corresponding TPO profile. As shown in previous work, when the Pt/KL catalyst gets poisoned by sulfur, there is a shift in the oxidation temperature of the carbonaceous deposits. We have previously observed similar shifts after sulfur poisoning [7] and ascribed them to the inhibition by sulfur of the catalytic action of Pt in the coke oxidation that takes place during TPO. As shown in Fig. 7a and in the previous work, as the sulfur poisoning progresses from 25 to 40 h, the high-temperature TPO peak grows in intensity. Therefore, the size of this high-temperature peak relative to the low temperature peak can be taken as an indication of the degree of sulfur poisoning of the Pt surface. In good agreement with the behavior exhibited in the catalytic activity measurements, it can be observed that the Ce-promoted catalyst is more tolerant to sulfur than the unpromoted Pt/KL. When comparing Fig. 7a and b, it is clear that the high-temperature peak for the Pt/KL catalyst after 40 h on stream is larger than that for the Pt/Ce-KL after 54 h.
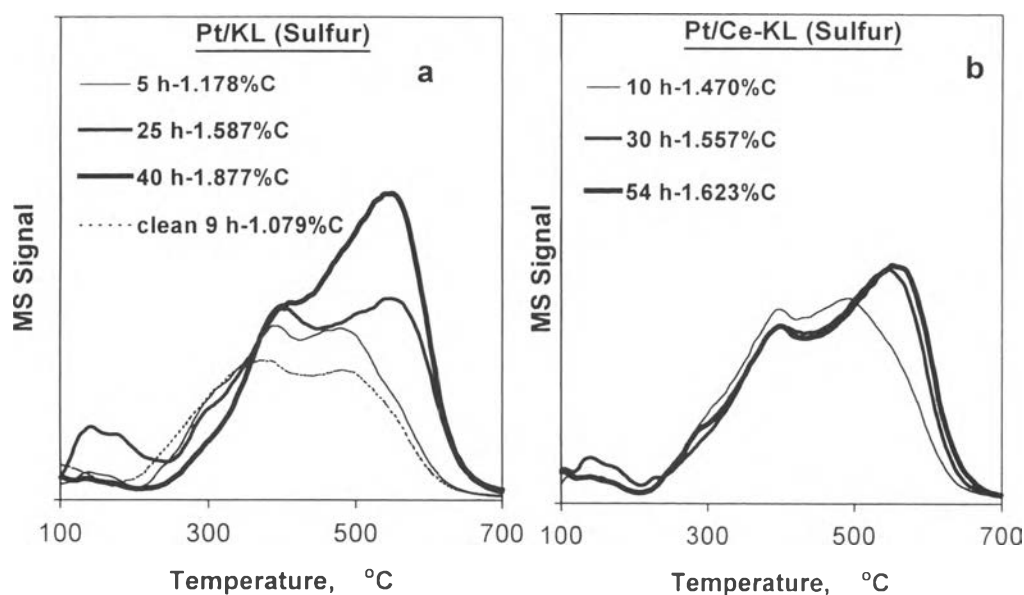

Fig. 7. TPO profiles of (a) Pt/KL and (b) Pt/Ce-KL spent catalysts after reaction at 500°C for different times on stream, using feed containing 2.5 ppm S. A sample run with a clean feed is included for each catalyst. The calculated amount of coke is included for each curve.

The TPO obtained on catalysts Pt/KL and Pt/Ce-KL after different exposure times to a "wet" feed containing n-hexane/hydrogen and 3 mol. % water are compared in Fig. 8a and b, respectively. Interesting differences are apparent in the overall trend observed for the two catalysts. In the first place, the changes in the TPO profiles as a function of time on stream are more pronounced on the unpromoted Pt/KL catalyst than on the Ce-promoted catalyst, not only in the total amount of coke, but also in the relative intensity of the TPO peak centered below 400°C. We have previously ascribed this peak to the oxidation of coke on metal particles located either on the outer surface of the zeolite or near the pore mouth, and therefore readily accessible for burning during the TPO. Clearly, this peak is more pronounced for the unpromoted Pt/KL catalyst exposed for the longest time to the water-containing feed, for which the most severe metal agglomeration can be expected. Since sulfur was not present in this case, the Pt particles did not lose their oxidation ability and allowed an easy elimination of coke during the TPO. Interestingly, the Ce-promoted catalyst exhibited reduced coke deposition in comparison to the unpromoted catalysts. This lower carbon formation trends were observed in the presence as well as in the absence of sulfur. The smaller size of the peak below 400°C is an indication of a lower degree of Pt agglomeration in this Ce-promoted sample.
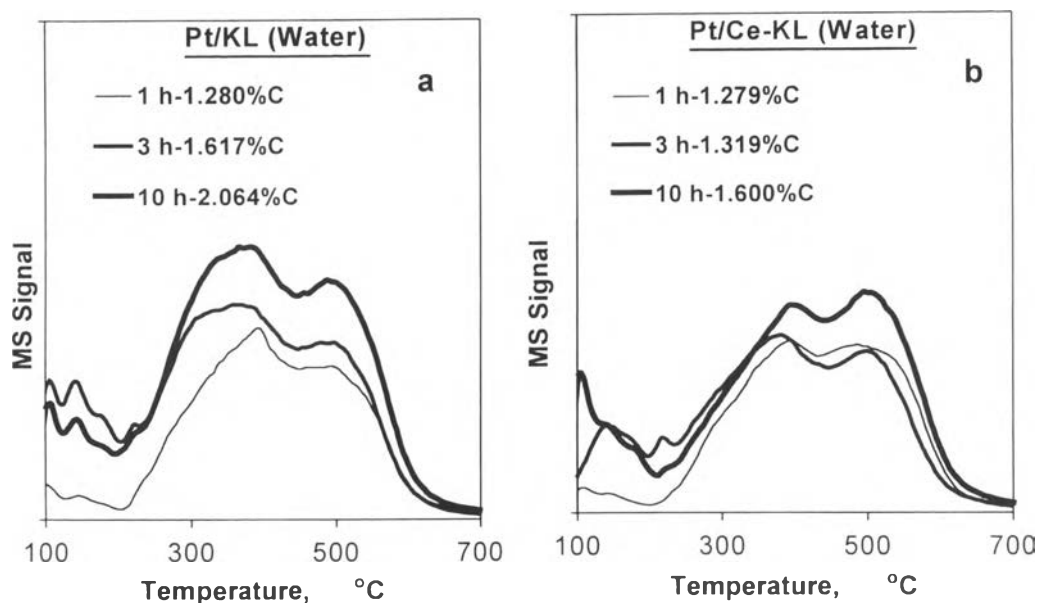
Fig. 8. TPO profiles of (a) Pt/KL and (b) Pt/Ce-KL spent catalyst after reaction at 500°C for different times on stream, using feed containing 3 mol. % H_2O. The calculated amount of coke is included for each curve.

Fig. 9a and b summarize the data from the TPO shown in Figs. 7 and 8. The amount of coke deposited on the two different catalysts as a function of time on a "dry" stream with 2.5 ppm S is compared in Fig. 9a. It is seen that even though the unpromoted Pt/KL initially forms less coke than the Ce-promoted sample, the opposite is true after 20 h on stream. At longer times, the unpromoted catalyst starts increasing the formation of coke much more rapidly than the Ce-promoted one. As advanced by Iglesia and coworker [29, 30], when Pt clusters are well dispersed inside the channels of the L-zeolite, they are protected from bimolecular collisions leading to coke formation. By contrast, Pt particles located outside the channels quickly become coked. In agreement with this view, our previous work [7] demonstrated that much more coke was deposited on IWI catalysts than on VPI catalyst, because even a well prepared IWI catalyst has some Pt particles outside the zeolite channels. The evolution of coke formation on the two catalysts can be explained by a greater resistance of the Ce-promoted catalyst to metal agglomeration under sulfur.
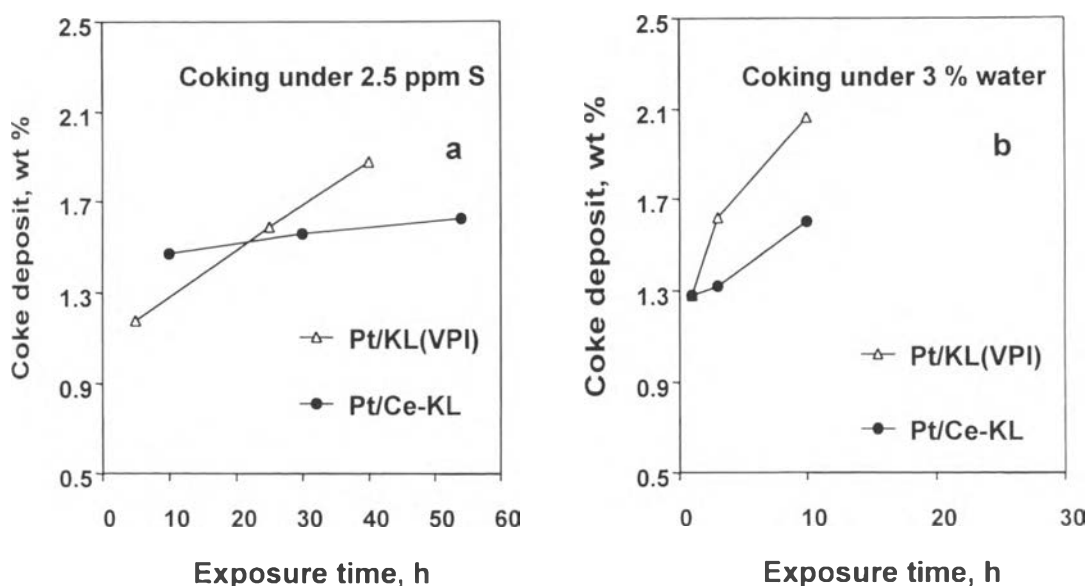
Fig. 9. Carbon deposits (wt. %) as calculated from integration of the TPO profiles of Fig. 8 expressed as a function of time on stream in (a) feed containing 2.5 ppm S and (b) feed containing 3 mol. % H_2O over Pt/KL and Pt/Ce-KL catalysts.

Similarly, Fig. 9b makes a comparison of the amount of coke deposits over the two catalysts after three different treatments in water-containing feed. First of all, it is observed that when the coke deposition took place in the presence of 3 mol. % water vapor, the amount of coke deposits greatly increased compared to the run with clean feed or even sulfur-containing feed, since after only a few hours on stream the carbon deposition was higher than that obtained after long reaction times under 2.5 ppm S (compare Fig. 9a and b). The second aspect to point out is the clear effect of Ce in inhibiting coke formation as a function of exposure time to a water-containing feed, which clearly agrees with the trend indicated.

2.4 EXAFS/XANES Analysis: The morphology of Pt clusters in the Pt/KL (VPI) and Pt/Ce-KL catalysts was investigated by EXAFS at liquid nitrogen temperature after reduction in H_2 at 500°C. Fig. 10 shows the Fourier transforms of the X-ray absorption data collected on the two samples. A slight difference was observed in the satellite peak to the left of the main Pt-Pt peak, but otherwise the spectra were almost identical, indicating that the Pt clusters in the two catalysts are very similar. In agreement with this qualitative observation, the quantification of the EXAFS data

done using the BAN software indicates that the structural parameters of the Pt clusters are very similar in both catalysts in the freshly reduced state (see Table 3).
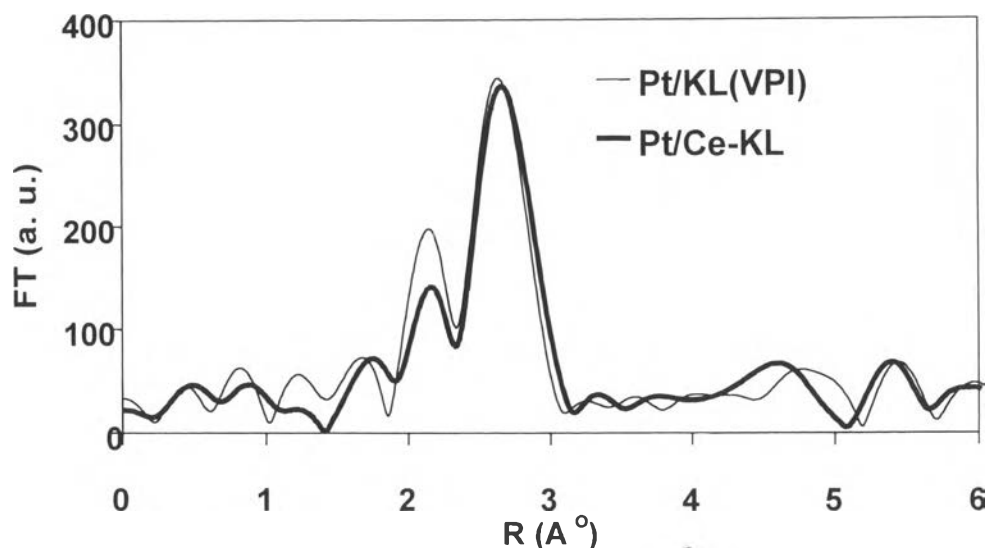

Fig. 10. Fourier transforms corresponding to the k^3-weighted Pt L_3-edge EXAFS spectra obtained at liquid nitrogen temperature on in situ reduced Pt/KL and Pt/Ce-KL catalysts.

Table 3

Structural parameters obtained from the fitting of the EXAFS data

Catalyst	R	ΔE_0	$\Delta\sigma^2$	CN/CN_0	Coordination Number (CN)
Pt/KL (VPI)	2.767	0.275	-0.00063	0.432	5.18
Pt/Ce-KL	2.757	2.295	-0.00094	0.450	5.40

The L_3 and L_2 absorption edges of Pt include intra-atomic transitions from the occupied 2p levels to unoccupied 5d levels. As pointed out by Ramaker et al. [31], there are significant differences among the transitions involved in each of the two edges. Specifically, as illustrated in Scheme 1, the L_3 edge includes transitions from the $2p_{3/2}$ level to the $5d_{5/2}$ and $5d_{3/2}$ levels, but the L_2 edge only includes a transition from the $2p_{1/2}$ level to the $5d_{3/2}$. In Fig. 11, the L_3 and L_2 absorption edges for Pt on the unpromoted and Ce-promoted Pt/KL (VPI) catalysts are compared to those of a

Pt foil. Obviously, the L_3 and L_2 spectra of a given sample have the same EXAFS oscillations. Therefore, the edges can be aligned in such a way to exactly superimpose the EXAFS part. This is the most reliable way to make comparisons of different absorption edges [31].
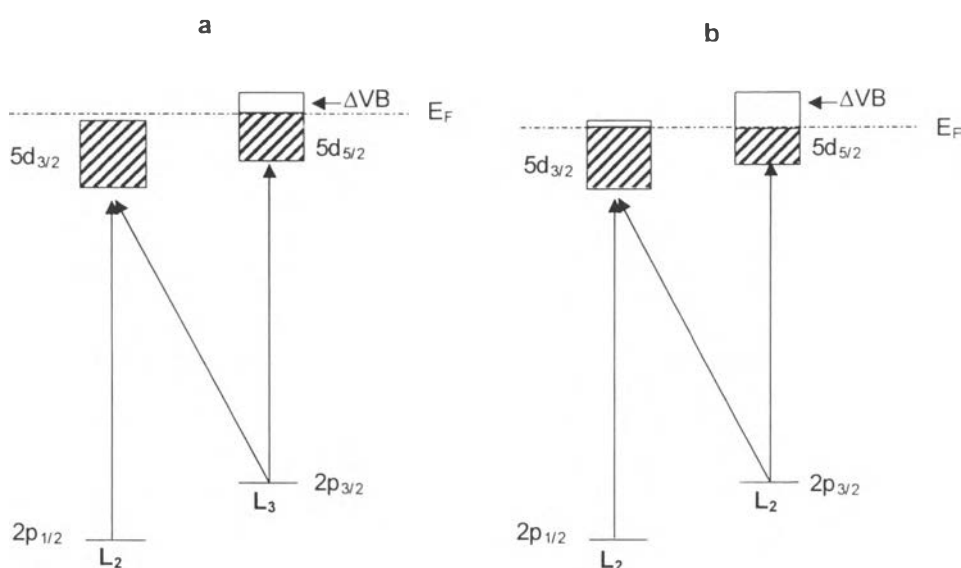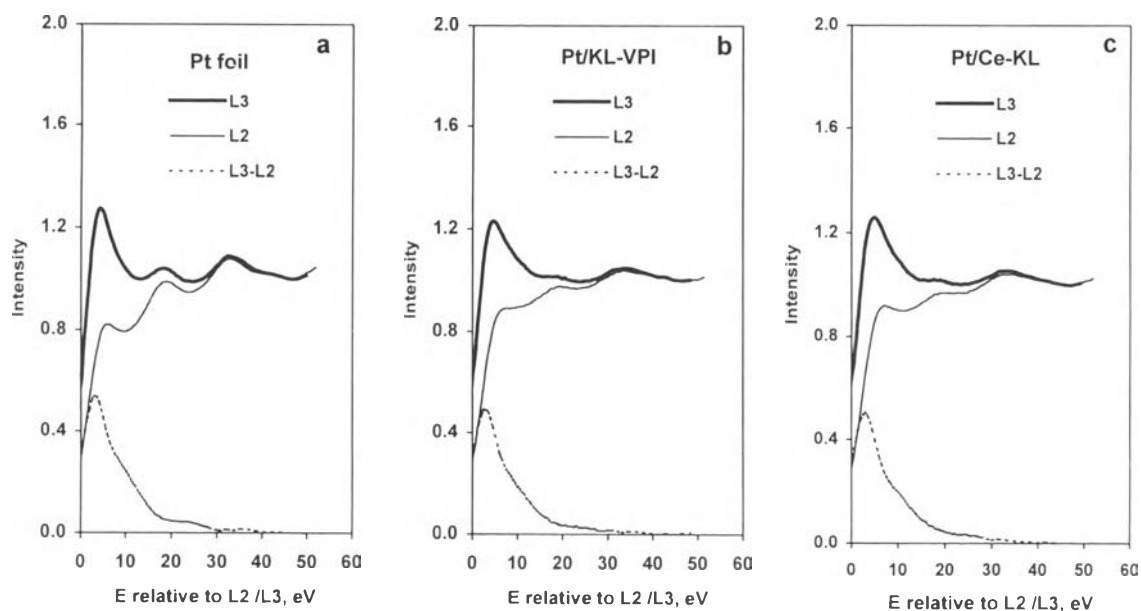

Scheme 1.

Fig. 11. XANES spectra of the Pt L_3 and L_2 edges obtained at liquid nitrogen temperature over a Pt foil, and Pt/KL and Pt/Ce-KL catalysts. Each set of spectra were aligned and normalized in order to match the EXAFS oscillations. The spectra of the catalysts were obtained after in situ reduction and flushing in He.

As can be observed for the L_2 edge, the first peak after the edge (white line), which is responsible for intra-atomic transitions is much smaller on the Pt/KL sample than on the Pt/Ce-KL or on the Pt foil. It has been proposed [31] that in very small Pt clusters, the $5d_{3/2}$ level falls below the Fermi level due to band narrowing, inhibiting the corresponding $2p_{1/2} \rightarrow 5d_{3/2}$ transition. The difference between the Pt/KL and the Pt foil can be interpreted in terms of the band narrowing, just due to particle size effects. However, the difference between the unpromoted Pt/KL and the Ce-promoted catalyst cannot be explained in those terms, since as shown in Table 3, both catalysts have comparably small Pt clusters. As clearly demonstrated in Fig. 12a, the difference between Pt/KL and Pt/Ce-KL, although small in comparison with the size of the absorption edge, it is large in comparison with the almost perfect match observed in the rest of the spectra. The enhanced absorption in the first peak after the edge would indicate that the $2p_{1/2} \rightarrow 5d_{3/2}$ transition occurs to a greater extent on the Ce-promoted catalyst than on the Pt/KL catalyst. This enhancement could be due to either an electron transfer from the Pt to the Ce-promoted zeolite, which would depopulate the $5d_{3/2}$ level, or a shift in the Fermi level, not associated with an electron transfer, but only due to a change in the Madelung potential of the zeolite around the Pt particle [32, 33]. Similar changes have been proposed for Pt supported on La^{3+}-containing zeolites [34]. Interestingly, since L_3 edges also include a transition to the $5d_{3/2}$ level, the same difference between Pt/KL and Pt/Ce-KL is carried along to this edge (see Fig. 12b).
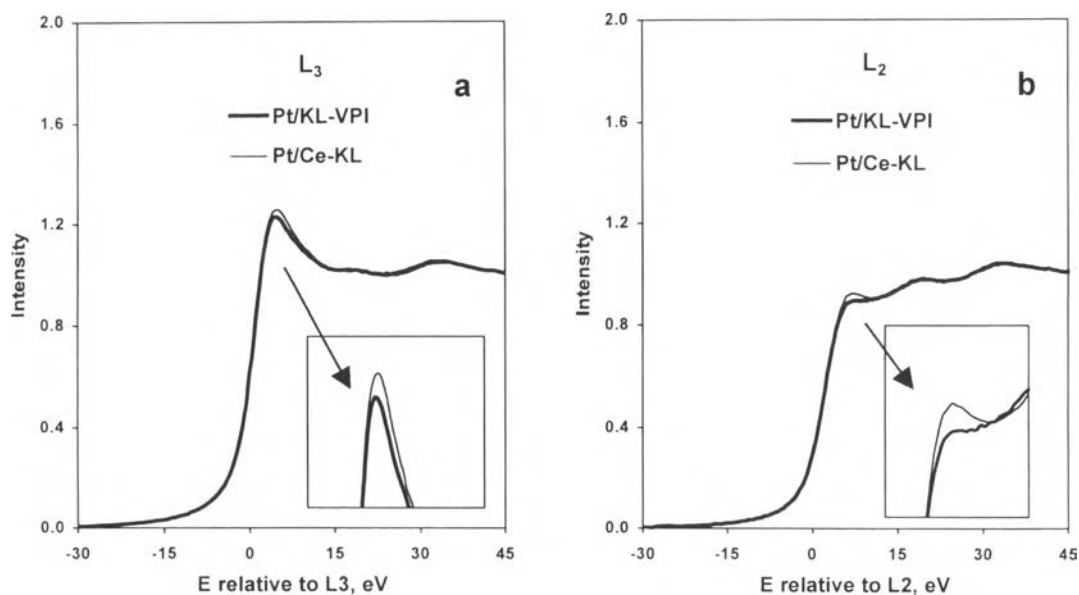
Fig. 12. Comparison for the XANES spectra of the (a) Pt L_2 and (b) Pt L_3 edges obtained in He at liquid nitrogen temperature after in situ reduction at $500^{\circ}C$ over the catalysts Pt/KL and Pt/Ce-KL. Inset emphasizes the differences in the white lines for the two catalysts.

Clearly, the analysis of the X-ray absorption edges indicates that some electronic differences may indeed exist in the state of Pt supported on the Ce-KL compared to that on the unpromoted KL zeolite. Although the Pt particle size and location inside the zeolite is very similar in the two zeolites, the presence of the RE seems to have influence on the electronic potential around Pt, which may be responsible for the observed enhanced stabilization of the small metal clusters.
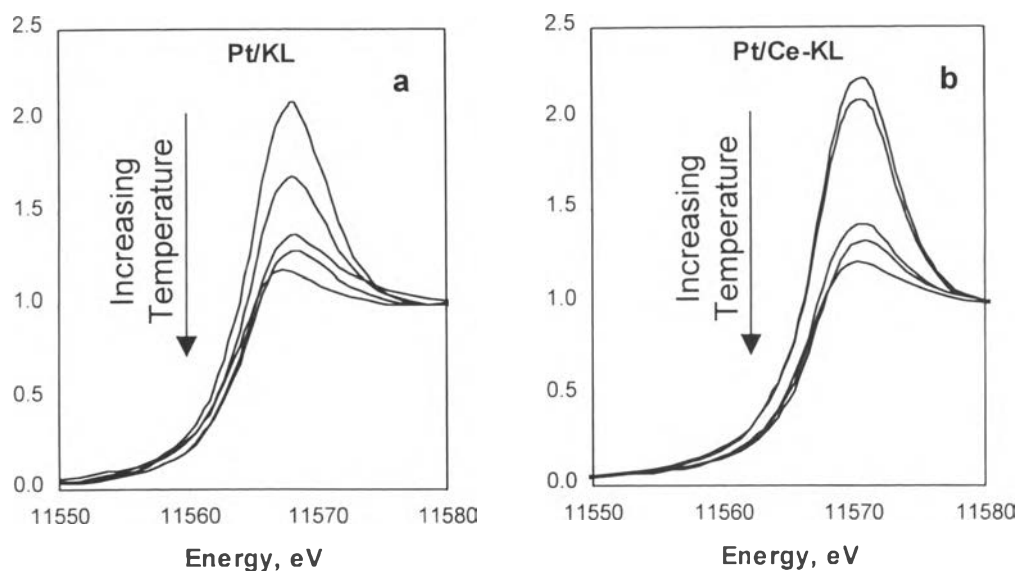
Fig. 13. XANES spectra of the Pt L₃ edges obtained under hydrogen as a function of temperature. More than 10 spectra were obtained for each sample at different temperatures (they are included in Fig. 14) but only five are shown here for the sake of clarity.
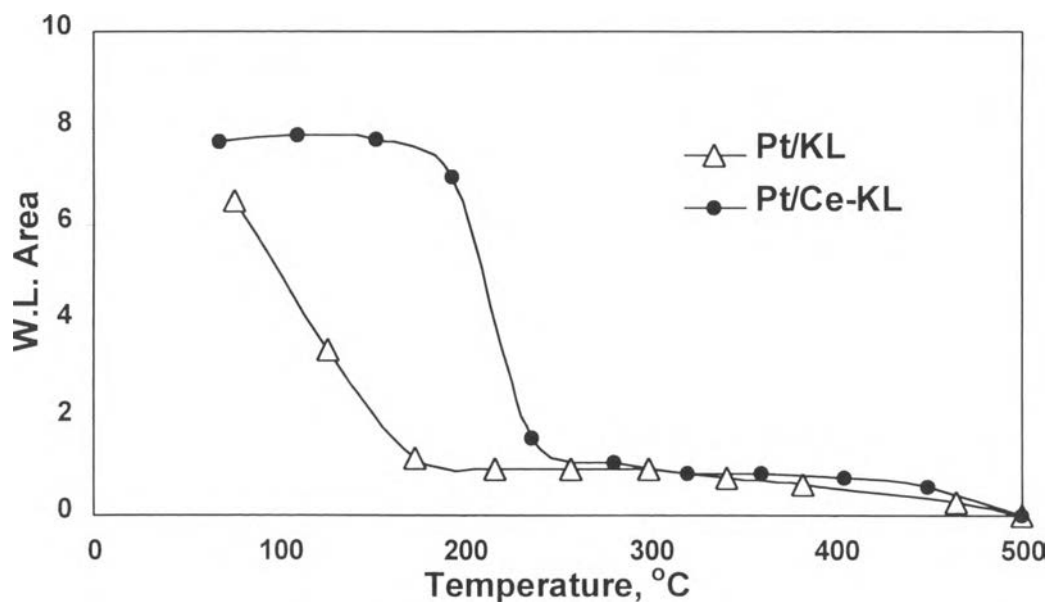

Fig. 14. Variation of the area under the first peak in the XANES spectra (white line) as a function of reduction temperature. The decrease in the size of the white line indicates the reduction of Pt.

To further investigate the effect of Ce in enhancing the interaction of Pt with the zeolite, we followed the evolution of the XANES spectra at increasing reduction temperatures to see whether the presence of Ce has any effect on the reducibility of the supported Pt. The XANES of the Pt L_3 was obtained after holding the sample under pure H_2 for 10 min at the indicated temperature. This comparison is illustrated in Fig. 13a and b, which show only a few of all the spectra taken. It is clearly seen that as the reduction proceeds the size of the white line in the L_3 edge decreases, reflecting the increase in the electron occupancy of the d levels when the Pt oxide is reduced to metallic Pt. The integrated area of the white line is a direct measurement of the oxidation state of Pt. The values of this area for all the measured spectra are summarized in Fig. 14 as a function of reduction time for the Pt/KL and Pt/Ce-KL catalysts. A clear difference is observed, showing that the presence of Ce in the zeolite greatly influences the reducibility of Pt. This clear metal-support interaction may in fact be responsible for the enhanced resistance to metal agglomeration displayed by the Ce-promoted catalysts under reaction conditions and in the presence of water vapor.

Conclusions

In summary, we have found that although under clean conditions the addition of Ce or Yb causes a decrease in activity, the stability of the catalysts is greatly enhanced by the presence of the rare earths. This enhanced stability is also observed after exposure to a water-containing feed. We have ascribed the improved stability to an inhibition in the agglomeration of Pt particles, which normally occurs on the unpromoted Pt/KL catalysts. This inhibition can be linked to metal-support interactions that are enhanced by the presence of rare earth oxides and are made evident by XANES analysis.

In the presence of sulfur, the addition of Ce and to a lesser extent Yb, significantly inhibit the deactivation of the catalysts. In this case, not only the more effective anchoring of the Pt clusters, but also the ability of Ce and Yb to capture sulfur may be responsible for the enhanced sulfur-tolerance.

Acknowledgements

References

1   J. R. Bernard, Proc. 5th Internat. Zeolite Confer., (L. V. C. Rees, editor) Heyden, London (1980) 686.

2   P. W. Tamm, D. H. Mohr, C. R. Wilson,. Stud. Surf. Sci. Catal. 38 (1988) 335.

3   T. R. Hughes, W. C. Buss, P. W. Tamm, R. L. Jacobson, in "Studies in Surface Science and Catalysis" Amsterdam 28 (1986) 725.

4   G. Jacobs, C. Padro, D. E. Resasco. J. Catal. 179 (1998) 43.

5   G. B. McVicker, J. L. Kao, J. J. Ziemak, W. E. Gates, J. L. Robbins, M. M. J. Treacy, S. B. Rice, T. H. Vanderspurt, V.R. Cross, A. K. Ghosh, J. Catal. 139 (1993) 48.

6   M. Vaarkamp, J. T. Miller, F. S. Modica, G. S. Lane, D. C. Koningsberger. J. Catal. 138 (1992) 675.

7   G. Jacobs, F. Ghadiali, A. Pisanu, C. L. Padro, A. Borgna, W. E. Alvarez. D. E. Resasco, J. Catal. 191 (2000) 116.

8   G. Jacobs, F. Ghadiali, A. Pisanu, A. Borgna, W. E. Alvarez, D. E. Resasco, Appl. Catal. 188, 79 (1999).

9   I. Manninger, Z. Zhan, X. L. Xu, Z. Paal, J. Mol. Catal. 65 (1991) 223.

10 I. Manninger, Z. Paal, B. Tesche, U. Klengler, I. Halasy, I. Kiricsi, J. Mol. Catal. 64 (1991) 361.

11   D. J. Ostgard, L. Kustov, K. R. Poeppelmeier, W. M. H. Sachtler, J. Catal. 133 (1992) 342.

12   X. Fang, F. Li, L. Lao, Appl. Catal. A 146 (1996) 297.

13   J. M. Grau, L. Daza, X. L. Seoane, A. Arcoya, Catal. Lett. 53 (1998) 161.

14   G. Larsen, G. L. Haller, D. E. Resasco, V. A. Durante, U. S. Patent 5,540,833 (1996).

15   D. E. Resasco, G. Jacobs, C. Padro, H. Liu. U. S. Patent 6,063,724 (2000).

16   X. Fang, F. Li, Q. Zhou, L. Luo, Appl. Catal. 161 (1997) 227.

17   G. Jacobs, W. E. Alvarez, D. E. Resasco, Appl. Catal. 206 (2001) 267.

18   S. B. Hong, E. Mielczarski, M. E. Davis, J. Catal. 134 (1992) 349.

19   M. Ballatreccia, R. Zanonin, C. Dossi, R. Psaro, S. Recchia, G. Vlaic, J. Chem. Soc. Farad. Trans. 91 (1995) 2045.

20   K. Poeppelmeier, T. Trowbridge, J.-L. Kao, US Patent 4,568,656 (1986).

21   S. J. Tauster, J. J. Steger, S. C. Fung, K. R. Poeppelmeier, W. G. Funk, A. A. Montagna, V. R. Cross, J. –L Kao, European Patent Appl. 145289 (1985).

22   D. E. Sayers, B. A. Bunker, in "X-ray Absorption: Principles, Applications, Techniques of EXAFS, SEXAFS, XANES", (D. Koningsberger, R. Prins, editors), Wiley, 1988, p. 211.

23   J. T. Miller, D. C. Koningsberger, J. Catal.162 (1996) 209.

24   J. W. A. Sachtler, G. A. Somorjai, J. Catal. 81 (1983) 77.

25   W. Insu, N. Kazutoshi, Met. Mater. Int. 7(2001) 241.

26   H. Shinji, S. Kazuyoshi, S. Yasushi, N. Toshiyuki, U. Yoichiro, M. Mamoru, B. Leo, J. Am. Ceram. Soc. 81 (1998) 145.

27   B. H. Davis, Catal. Today 53 (1999) 443.

28   A. Y. Stakheev, E. S. Shpiro, N. I. Jaeger, G. Schulz-Ekloff, Catal. Lett. 34 (1995) 293.

29   E. Iglesia, J. E. Vaumgartner, Proc. IX Internat. Zeolite Conf., Montreal, 1992.

30   E. Iglesia, J. E. Baumgartner, Proc. 10th Internat. Congr. on Catalysis, Budapest, 1992, p.993.

31   D. E. Ramaker, B. L. Mojet, M. T. Garriga Oostenbrink, J. T. Miller, D. C.

Koningsberger, Phys. Chem. Chem. Phys. 1 (1999) 2293.

32   W. Grunert, M. Muhler, K.-P. Schroder, J. Sauer, R. Schlögl, J. Phys. Chem. 98 (1994) 10920.

33   D.C. Koningsberger, J. de Graaf, B.L. Mojet, D.E. Ramaker, J.T. Miller, Appl. Catal. A, 191 (2000) 205.

34   Y. Okamoto, M. Ogawa, A. Maezawa, T. Imanaka, J. Catal. 112 (1988) 427.